International Journal of General Engineering and Technology (IJGET)
ISSN(P): 2278-9928; ISSN(E): 2278-9936
Vol. 3, Issue 4, July 2014, 9-16

International Academy of Science, Engineering and Technology
Connecting Researchers; Nurturing Innovations

THERMAL ANNEALING AND UV INDUCED EFFECTS ON THE STRUCTURAL AND OPTICAL PROPERTIES OF CAPPING FREE ZNS NANOPARTICLES SYNTHESIZED BY CO-PRECIPITATION METHOD

A. A. OTHMAN[1], M. A. OSMAN[2], M. H. WAHDAN[3] & A. G. ABED-ELRAHIM[4]

[1,2,4]Department of Physics, Faculty of Science, Assiut University, Assiut, Egypt

[3]Department of Chemistry, Faculty of Science, Assiut University, Assiut, Egypt

ABSTRACT

Capping free Zinc Sulphide nanoparticles were synthesis from aqueous solutions of Zinc Chloride ($ZnCl_2$) and Sodium Sulphide (Na_2S) in air at 70^oC by co-precipitation method. The as-prepared and annealed samples were characterized by X-ray diffraction (XRD), UV-Vis absorption, scanning electron microscope (SEM), transmission electron microscope (TEM) and selected area electron diffraction (SAED). Analysis of XRD pattern indicates that the as prepared and annealed samples up to 300^oC ZnS nano-crystallites have cubic zinc blend structure. Furthermore, annealing at 550^oC, results in partial conversion of the initially cubic ZnS, to ZnS and ZnO Hexagonal phases as revealed by XRD patterns. SAED pattern for as-prepared ZnS reveals the polycrystalline nature. Furthermore, the lattice parameters determined from (XRD) and (SAED) patterns are in good agreement. Annealing of the ZnS nanoparticles in air in the temperature range, 150 – 550^oC, leads to the increase in crystallite size from 2.14 to 18 nm accompanied by decrease in optical band gap (E_g^{opt}) from 3.98 to 3.3eV, for the as prepared and sample annealed at 550^oC respectively. Analysis of TEM and SEM Images indicates that the ZnS nanoparticles tend to be nearly spherically shaped with narrow size distribution. Different times UV irradiation of ZnS aqueous solution results in increase in optical energy gap with the irradiation time. The observed photo brightening is explained in terms of the formation of $ZnSO_4$ passivation layer via photon-assisted chemical reaction.

KEYWORDS: Annealing, Optical Absorption, Photo-Brightening, UV-Induced, XRD, Zns Nanoparticles

INTRODUCTION

Nanometer sized Semiconductor nanoparticles have received great attention due to their exciting novel physical and chemical properties which differs from those of the corresponding bulk materials [1-3]. This difference is due to the confinement of electrons and holes in a small volume and to the fact that the number of surface atoms is comparable to the number in the interior of the nanoparticles [4]. Nanoparticles have larger surface to volume ratio and surface atoms are bound by weak forces because of missing neighbors, which leads to high surface reactivity. Semiconductor Nanoparticles can be prepared by different methods, like solid state reaction [5], hydrothermal synthetic method[6], microwave heatig[7], ultrasonic method [8].

Zinc sulfide is one of the most important II -IV semiconductors with bulk direct band gap energy 3.6eV [9] for cubic phase. It is a versatile and promising semiconductor having novel fundamental properties and diverse applications such as ultraviolet light sensors [10], efficient UV light emitting diodes [11], optoelectronic devices [12], novel bio-molecular applications, such as DNA detection [13], and electroluminescent applications [14]. In this paper, ZnS

nanoparticles were synthesized via chemical precipitation method without stabilizing agent. This makes possible to study the real properties of the nanoparticles. Annealing and UV irradiation induced effects on structure and optical behavior of capping free ZnS nanoparticles were studied. The samples were characterized by using X-ray diffraction (XRD), transmission electron microscopy (TEM), and UV-Vis Spectroscopy, Scanning electron microscopy (SEM).

EXPERIMENTAL DETAILS

ZnS nanoparticles were prepared from aqueous solutions of $ZnCl_2$ (50 ml, 0.1 M) was stirred at 200 rpm for 2h at temperature 70^{o}C. The milky solution centrifuged at 2500 rpm for 15 min then washed three times by double distilled water and by ethanol. The obtained product was dried in oven at 100^{o}C for 1h.The chemical reaction takes place as follows:

$$ZnCl_2 + Na_2S \xrightarrow[stirr.200\ rpm]{70\ ^oC} ZnS + 2NaCl \quad (1)$$

The structure of the obtained ZnS nanoparticles were characterized using Phillips x-ray diffraction (PW 1700 X-ray diffractometer with Cu K_α radiation λ=1.5405 A^o).The surface morphology was analyzed by scanning electron microscope (SEM) (JEOL JSM-5400 LV, with operating voltage=20kV).Selected area electron diffraction (SAED) (JEM 100 CXII with operating voltage = 80 kV) was used to examine the crystalline nature of the material. The optical band gap (E_g^{opt}) of ZnS nanoparticles dispersed in double distilled water was determined by analysis of the absorbance spectra recorded using double beam spectrophotometer (Perkin Elmer lambda 750). Annealing of the sample was carried out in research oven in the temperature range 150 - 550^{o}C. UV irradiation experiment was done by using UV research lamp (Minera- light, San Gabriel, CA).

RESULTS AND DISCUSSIONS

Annealing Induced Effect on Zns Nanostructure

Structural properties of the as-prepared ZnS nanoparticles are determined by x-ray diffraction. Figure (1) shows the XRD patterns of the as prepared and annealed ZnS nanoparticles samples in the range 150-550^{o}C. The broadening of the XRD peaks shows the typical nanocrystalline character of the samples. The XRD for as prepared ZnS exhibits three prominent diffraction peaks at 2θ values of 28.7^o, 47.72^o and 56.42^o. The deduced inter-planar distances $d_{(111)}$ =3.108 Å , $d_{(220)}$ =1.904 Å and $d_{(311)}$=1.63 Å, as well as the corresponding lattice parameter a = b = c = 5.387 Å , are in good agreement with the (111), (220) and (311) crystalline planes of the ZnS cubic phase, standard card (JCPDS no. 01-072-4841). The Crystallite size (D_S) was calculated using the following Scherrer formula [15]:

$$D_S = \frac{k\lambda}{\beta \cos\theta} \quad (2)$$

k is a shape constant = 0.89, λ is the x-ray wavelength, β is the full width at half maximum (FWHM) of the diffraction peak and θ is the angle of diffraction. The increase in annealing temperature leads to increase in crystallite size, due to the reduction of structural defects, which can be observed from narrowing of the diffraction peaks. Furthermore, partial phase transition from ZnS cubic structure to ZnS hexagonal structure takes place at annealing temperature T_a = 400^{o}C, on the contrary, the bulk transforms from cubic to hexagonal structure at 1020 °C.

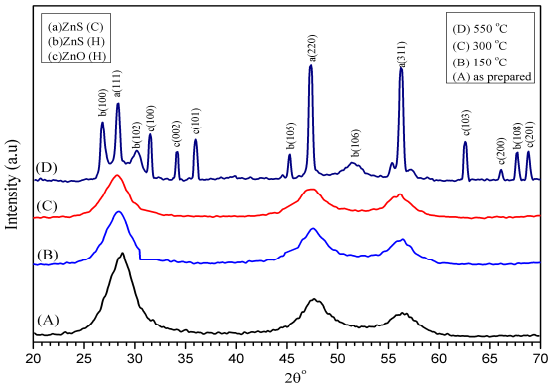

Figure 1: XRD of as Synthesizes and Annealed Zns Nanoparticles

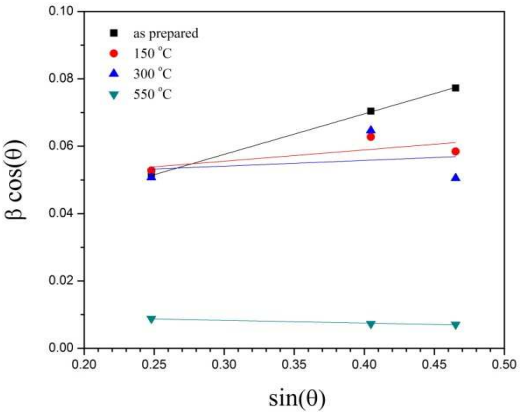

Figure 2: B Cosθ versus Sinθ According to W-H Equation for as Synthesized and Annealed Zns

Similar behavior was observed by B. Qadri, et al [16]. At T_a = 550°C, there will be mixed phases of ZnS cubic and hexagonal structures plus ZnO hexagonal structure. The calculated inter-planar distances $d_{(111)}$ =3.127 Å, $d_{(220)}$ =1.911Å and $d_{(311)}$=1.63Å corresponds to lattice parameter a = b = c = 5.416 Å for the ZnS Cubic structure ,which in agreement with standard card [[JCPDS no. 04-015-3042], Furthermore, inter-planar distances $d_{(100)}$ =2.845 Å, $d_{(002)}$ =2.626Å and $d_{(311)}$=2.46Å correspond to lattice parameter a = b = 3.285 Å and c = 5.252 Å for the hexagonal structure ZnO. Figure 2 shows Williamson-Hall (W-H) plot, equation (3), based on the uniform strain deformation model (USDM) [16]:

$$\beta\cos\theta = \frac{k\lambda}{D_w} + 4\varepsilon \sin\theta \qquad (3)$$

The lattice strain ε and the crystallite size D estimated from Williamson - Hall equation (3) are given in table (1). The decrease in interfacial defects and dangling bonds and the enhancement of crystallinity (the increase of D) causes reduction in the surface tension σ, ($\sigma = \sigma_\infty + \frac{constant}{D}$); σ_∞ is the surface tension at D ∞w. The larger crystallite size D, the weaker the surface tension σ to drive the surface reconstruction or modification [17], hence; the decrease of internal strain ε with the increase of annealing temperature (T_a). On the other hand thermal annealing may assist the aggregation of individual small ZnS nano particles to form larger crystallites, which may result in the decrease in optical band gap E_g^{opt}

Figure3 (a,b) and figure 4 shows TEM image and the corresponding histogram and SEM image for the as prepared ZnS nanoparticles. We can observe that the particle edges are ambiguous, which is probably due to the presence of aggregation of small nanocrystals to produce a large irregular agglomerates.

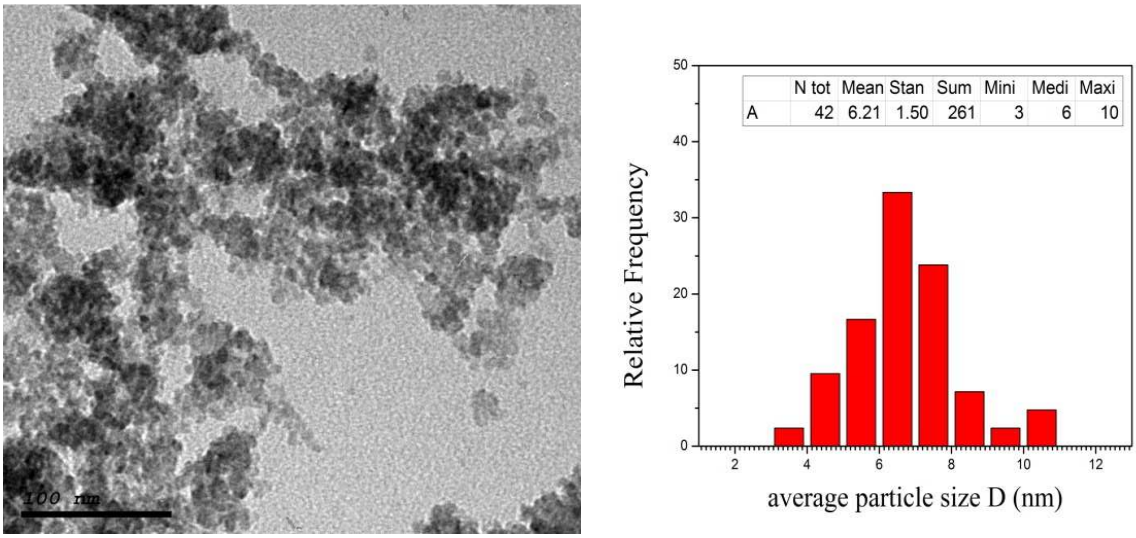

Figure 3: (A) TEM Micrograph of the as Synthesized Zns Nano Particles, (B). Histogram of Particle Sizedistribution

Furthermore, the surface morphology exhibits nearly spherical shape, analysis of TEM Images using statistical method give the average particle size which equal to 6.2 nm with st.dev.≈ 1.5 < 7%, which indicates the mono-disperse nature of ZnS nanoparticles.

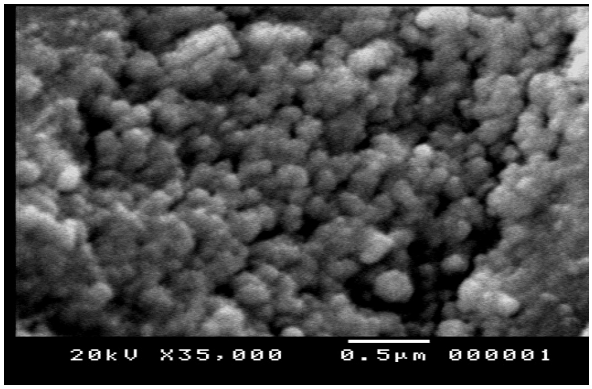

Figure 4: SEM Micrograph of the as Synthesized Zns Nanoparticles

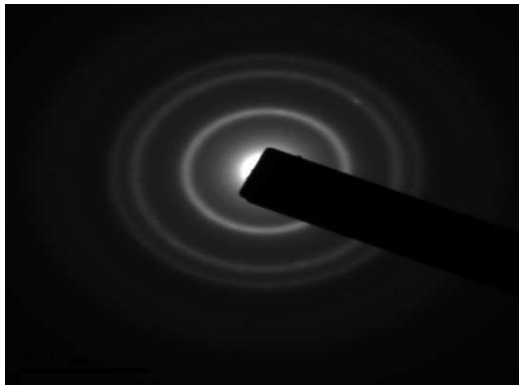

Figure 5: SAED Pattern of the as Synthesized Zns Nano Particles

SAED image of the as prepared ZnS nanoparticles, figure 5, reveals three concentric diffraction rings, of the prominent planes corresponding to inter-planar distance $d_{(111)}$ =3.1Å, $d_{(220)}$ =1.89Å and $d_{(311)}$ =1.63Å, and lattice constant a=b=c=5.37Å of cubic ZnS structure. The obtained values agree well with XRD results and are in a good agreement with the standard card (JCPDS: 01-072-4841).

Table 1: Dependence of Nanocry stallite Size D, Lattice Constant, Unit Cell Volume, Lattice Strain Ɛ and Energy Gap Values for Zns Nano particles at Different Annealing Temperature

Annealing Temperature T(^{O}c)	D_S (Nm)	D_{W-H} (Nm)	Lattice Constant A (A^o)	Unit Cell Volume V (A^{o3})	Lattice Strain Ɛ	E_g^{opt} (Ev)
As prepared 35	2.14	6.4	5.3874	156.364322	0.03008	3.98
150	2.4	2.95	5.4393	160.92704	0.0076	3.83
300	2.5	2.75	5.4733	163.9637	0.00355	3.71
550	18	12.8	5.45757	162.55411	0.00201	3.3

Annealing Effect on Optical Behavior

Figure. (6) shows the optical absorption behavior of the as prepared and annealed ZnS samples annealed at different annealing temperatures. The optical gap E_g^{opt}, can be determined by plotting $(\alpha h\nu)^2$ versus hν according to Tauc' s Relation [18]:

$$(\alpha h\nu) = A\,(h\nu - E_g^{opt})^n \quad (4)$$

A is the ordering parameter, hν is the photon energy, and E_g^{opt} is the optical band gap of the nanoparticles. The power n is a constant that can take different values depending on the type of electronic transition. For allowed direct transition n =1/2, for forbidden direct transition n =3/2, for allowed indirect transition n = 2, and for forbidden indirect transition n = 3. The values of E_g^{opt} were determined by extrapolation of the least square linear regions of the plot of $(\alpha h\nu)^2$ versus hν to the value $(\alpha h\nu)^2$ = zero, table (1).

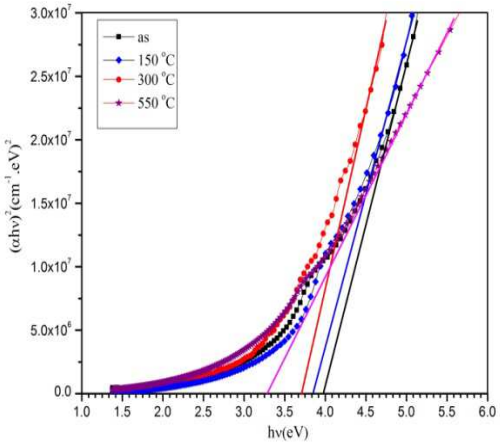

Figure 6: $(Ahv)^2$ Versus Hv For Zns Nanoparticles Annealed at Different Temperature

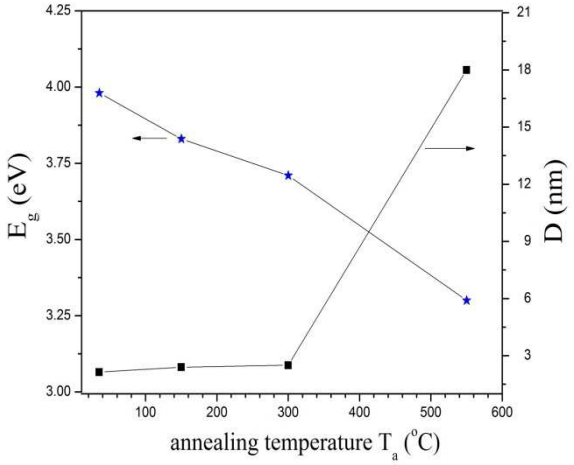

Figure 7: Variation of E_g^{optT} and Crystallite Size D as Function of Annealing Temperature

Figure 7 shows the variation of optical band gap and crystallite size with annealing temperature, the optical band gap decreases with increasing the annealing temperature due to the reduction of quantum confinement as a result of increasing particles size.

UV Irradiation Induced Effect on Optical Energy Gap

The optical absorption and transmittance spectra of the nano ZnS dispersed in double distilled water recorded in the range 200 - 900 nm, for as-prepared and UV illuminated sample (times 0 - 60 min.) are shown in figures (8,9). The absorption edge is observed to be blue shifted compared to bulk ZnS. As the UV illumination time increases, the absorption edge shifts to lower wavelength, and the absorption intensity decreases (T% increases compared to un illuminated ZnS solution). This blue shift in the optical absorption gap for different illumination is shown in figure (10)

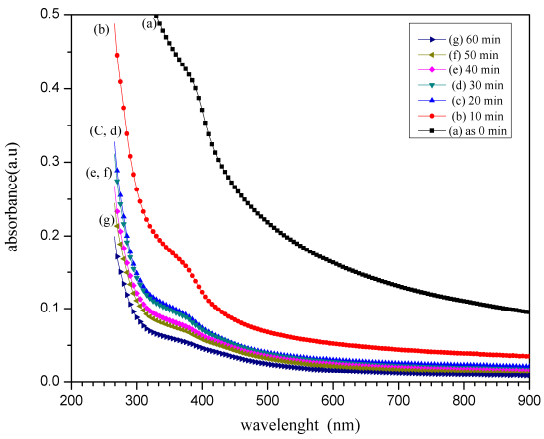

Figure 8: Absorption Spectra of Aqueous Solution of Zns Nanoparticles Irradiated with Uv for Different Times

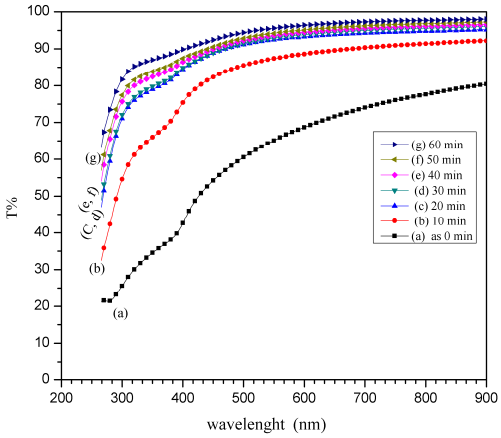

Figure 9: Transmittance Spectra of Aqueous Solution of Zns Nanoparticles Irradiated with Uv for Different Times

Figure (11) refers to the decrease in the particle size D and the increase in the optical gap to higher energy, as a function of UV irradiation times. Surface properties have significant effects on the optical properties of nanoparticles and a large portion of atoms are located at or near their surfaces. These surface atoms usually have unsaturated or dangling bonds. Hetero-structural interfaces also contain strain-induced defects[20], [21]. The observed increase in the optical band gap (photo-brightening) with increasing UV illumination time, figure (11), may be attributed to one or more of the following reasons:

- Increasing UV irradiation time may leads to the reduction of defects and the unsaturated dangling bonds.
- UV illumination of ZnS nanoparticles aqueous solution in ambient air may be accompanied by photo-oxidation of ZnS to ZnSO4 which act as passivation or capping layer [20] due to a photon-assisted chemical reaction between ZnS nanoparticles and oxygen in water. Hence, the increase in illumination time leads to decrease in particle size, accompanied by increase in optical band gap. An evidence for the photo oxidation was found in measuring the excitation spectra of nano ZnS:$Mn^{+}2$, measured at different UV illumination times [22], where both the maximum and the onset of the excitation spectra shift to shorter wavelength (i.e blue shifted).

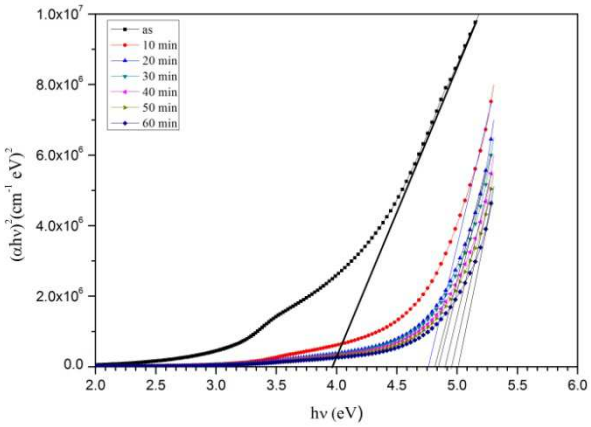

Figure 10: Plot of $(\alpha h\nu)^2$ Versus Hν for of Aqueous Solution of Zns Nanoparticles Irradiated With UV Light for Different Times

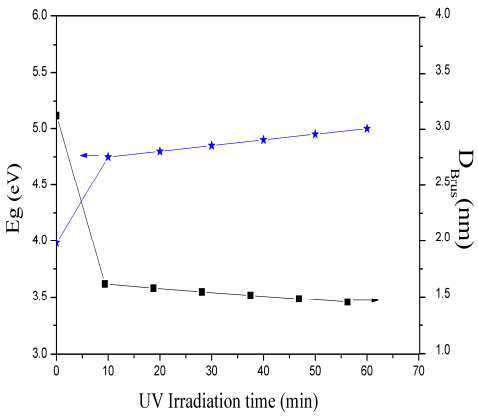

Figure 11: E_g^{opt} and Particle Size D, as Functions of Zns Nanoparticles Irradiated with UV Light for Different Times

The band gap shift E_g with respect to bulk value has been estimated and utilized for particle size estimation by using Effective mass approximation 'EMA' according to the following Brus's equation:

$$\mathbf{E_g^{opt}}\text{ (nano)} = \mathbf{E_g^{opt}}\text{ (bulk)} + \frac{\mathbf{h^2}}{\mathbf{8\mu d^2}} - \frac{\mathbf{1.8e^2}}{\boldsymbol{\epsilon}\mathbf{d}} \quad (5)$$

$\boldsymbol{\epsilon}$ = 8.76 is the relative dielectric constant [19] and $\boldsymbol{\mu = m_e^* m_h^*/(m_e^* + m_h^*)}$ is the reduced electron - hole effective mass. m^*_e = 0.34 m_o and m^*_h =0.23 m_o are the effective masses of electron and hole respectively and m_o is rest electron mass, $\boldsymbol{E_g^{opt}}$ (bulk) is the energy gap of the bulk ZnS (≈3.6 eV), and E_g (nano) is the energy gap of the as prepared ZnS nanoparticles.

Table 2: E_g^{opt} , ΔE_g^{opt}, and Particle Size D, for Zns Nanoparticles as Function of Irradiation Time

Uv Irradiation Times	0 Min	10 Min	20 Min	30 Min	40 Min	50 Min	60 Min
E_g^{opt}(eV)	3.98	4.75	4.8	4.85	4.9	4.95	5
ΔE_g^{opt}(eV)	0.28	1.05	1.1	1.15	1.2	1.25	1.3
D (nm)	3.13	1.62	1.58	1.55	1.51	1.48	1.45

CONCLUSIONS

Capping free Zinc Sulphide nanoparticles are synthesized in air at 70°C by Co-precipitation method to investigate annealing and UV Irradiation induced effects on the structure and optical properties. Main conclusions drawn from the present study are:

- Annealing at 550 °C partially converts the initially cubic ZnS into ZnS and ZnO Hexagonal phases. This phase transition occurs at 470°C lower than the corresponding phase transition temperature for the bulk ZnS (1020°C)
- Annealing of the samples results in the increase in the particles size; hence the decrease in the optical band gap E_g^{opt} from 3.98 eV to 3.3 eV(red shift).
- UV irradiation induces photo-brightening, i.e the increase of E_g^{opt} from 3.98 eV to 5 eV (blue shift) may be attributed to the formation of $ZnSO_4$ passivation layer via photon assisted chemical reaction.
- The present study indicates that annealing and UV irradiation are strong tools for tuning optical properties of ZnS which is useful in optoelectronic devices and other applications.

REFERENCES

1. A. P. Alivisatos, Science vol 271, no. 5251, (1996), 933-937. (b) L. Brus, J. Phys. Chem. 90, 2555 (1986).
2. Y. Wang and N. Herron, J. Phys. Chem. 95, 525-582(1991).
3. H. Weller, Adv. Mater. 5, 88(1993).
4. R. Sharma, S. J. Dhoble, D. P. Bisen, N. Brahme, and B. P. Chandra, Int. J. Nanoparticles, 4(2011) 64–76.
5. (a) S. Sain, S. K. Pradhan, J. Alloys Compd. 509(2011), 4176-4184.

   (b) Mohd Mubashshir Hasan Farooqi, R.K. Srivastava, S. G Prakash, AIP conference proceedings 1536(2013)179.
6. K. Byrappa, T. Adschiri, Prog. Cryst. Growth Charact. Mater, 53 (2007), 117-166.

7. (a) I. A. Lopez, A.Vazquez, and I. Gomez, Revista Mexicana de Fisica 59 (2013), 160-164.
(b) Robina Shahid, Muhammet S. Toprak, Mamoun Muhammed, J. Solid State Chem. 187 (2012)130-133.
8. (a) Veronica Sáez and Timothy J. Mason, Molecules, 14(2009),4284-4299.
(b) Matjaz Kristl, Irena Ban, Anita Danc, Valerija Danc, Miha Drofenik. Ultrason. Sonochem. 17(2010), 916-922.
9. Ni, Y., Yin, G., Hong, J., Xu, Z. Mater. Res. Bull. 39(2004), 1967-1972.
10. Xiaosheng Fang, Yoshio Bando, Meiyong Liao, Tianyou Zhai, Ujjal K. Gautam, Liang Li, Yasuo Koide and Dmitri Golberg, Adv. Funct. Mater. 20 (2010), 500–508.
11. Rui Chen, Dehui Li, Bo Liu, Zeping Peng, Gagik G. Gurzadyan, Qihua Xiong, Handong Sun, Nano Lett. 10 (2010) 4956–4961
12. M. Kastner, Artificial atoms, Phys. Today 46 (1993), 24.
13. Y. Li, J. Chen, C. Zhu, L. Wang, D. Zhao, S. Zhuo, Y. Wu, Spectrochim. Acta A 60 (2004) 1719–1724.
14. V. Colvin, M. Schlamp, A. P. Alivisatos, Nature 370 (1994) 354.
15. B.D. Cullity Deceased and S.R. Stock, Elements of X-Ray Diffraction (3rd ed.), *2001 by Prentice Hall*
16. S. B. Qadri, E. F. Skelton, D. Dinsmore, J. Yang, H. F. Gary, and B. R. RAtna, Phys. Rev. B, no.13, 60 (1999), 9191-9193.
17. Jia-Yu Zhang, Xiao-Yong Wang, Min Xiao, L. Qu and X. Peng, Appl. Phys. Lett. 81(2002), 2076
18. J. Tauc, A. Menth, Non-Cryst. Solids 8(1972), 569.
19. P. K. Ghosh, S. Jana, S. Nandy, and K. K. Chattopadhyay, Mater. Res. Bull., 42 (2007) 505.
20. D. R. Jung, J. Kim, and B. Park, J. Appl Phys Lett, vol. 96, 2010.
21. A B. Cruz, Q. Shen, and T. Toyoda, Thin Solid Films, vol. 499, pp. 104–109, 2006.
22. A Meijerink and A. A. Bol, phys. stat. sol., vol. 224, no. 1, pp. 291–296, 2011.